Colloids and Surfaces B: Biointerfaces 68 (2009) 93–97

Contents lists available at ScienceDirect

Colloids and Surfaces B: Biointerfaces

journal homepage: www.elsevier.com/locate/colsurfb

Improved direct electron transfer and electrocatalytic activity of horseradish peroxidase immobilized on gemini surfactant–polyvinyl alcohol composite film

Lihong Liu, Faqiong Zhao, Liqin Liu, Jing Li, Baizhao Zeng*

Department of Chemistry, Wuhan University, Wuhan 430072, PR China

ARTICLE INFO

Article history:
Received 6 June 2008
Accepted 17 September 2008
Available online 26 September 2008

Keywords:
Horseradish peroxidase
Cationic gemini surfactant
Polyvinyl alcohol
Electrocatalysis
Hydrogen peroxide

ABSTRACT

The voltammetric and electrocatalytic behavior of horseradish peroxidase (HRP) immobilized on a cationic gemini surfactant (i.e. $C_{12}H_{25}N(CH_3)_2$–$C_{12}H_{24}$–$N(CH_3)_2C_{12}H_{25}Br_2$, C_{12}–C_{12}–C_{12})–polyvinyl alcohol (PVA) composite film-coated glassy carbon electrode (GCE) has been studied. It is found that on the novel composite film HRP presents excellent electroactivity and can exhibit a pair of well-defined voltammetric peaks in 0.10 M pH 7.0 phosphate buffer solution (PBS). The immobilized HRP also presents good bioelectrocatalytic activity, and it can catalyze the reduction of oxygen (O_2), hydrogen peroxide (H_2O_2), nitrite ion (NO_2^-) and trichloroacetic acid (TCA). For H_2O_2 the catalytic current is linear to its concentration in the range of 0.195–97.5 μM, and the detection limit is down to 6.5×10^{-8} M. The response shows Michaelis–Menten feature and the apparent Michaelis–Menten constant is estimated to be 110.5 μM. Similarly, the electrode can sense NO_2^- and TCA. In addition, it is observed that the spacer group of gemini surfactant affects the electroactivity of HRP significantly. A spacer group with higher flexibility and hydrophility is favorable to the electron transfer of HRP. UV–vis spectrum indicates that the structure of HRP in the PVA–C_{12}–C_{12}–C_{12} film is similar to that of native HRP. Thus the C_{12}–C_{12}–C_{12}–PVA composite possesses good biocompatibility and has promising application in fabricating biosensor and bioelectronics.

1. Introduction

In recent years, much attention has been paid to the direct electron transfer (DET) of redox enzymes [1–4]. It is thought that the related study can lay an electrochemical basis for understanding enzyme system, which concerns enzyme structure, redox transformation and catalytic mechanism. However, the heterogeneous electron transfer of redox enzymes is generally rather slow because their electroactive prosthetic groups are usually embedded in the molecules [5]. Therefore, to enhance their heterogeneous electron-transfer rate is one of the main purposes in the electrochemical study of enzymes. Research shows that through improving the microenvironment around enzyme molecules their direct electron transfer can be effectively promoted [6–8]. Hence, various materials were tested for such purpose. Because horseradish peroxidase (HRP) has good stability and is commercial available, it is considered an ideal model molecule and is usually adopted in such studies [9,10]. For example, Liu et al. studied the effect of dipalmitoylphosphatidic acid on the direct electron transfer of HRP [9]; Chen and Dong reported the direct electron transfer of HRP in sol–gel-derived ceramic-carbon nanotube nanocomposite film [10]; Zeng and coworkers declared that ionic liquids could promote the electron transfer of HRP [11]. In addition, it was found that conventional surfactants could enhance the heterogeneous electron-transfer rate of HRP [12].

Gemini surfactants are a new type of surfactant, which contains two or more hydrophobic alkyl chains and two or more hydrophilic groups. They show many unique physical–chemical properties such as lower critical micelle concentration (CMC), higher efficiency in lowering the surface tension of water and the interfacial tension between water and oil, and better solubility in water. Thus, they received considerable attention [13,14]. So far, the series of gemini surfactant studied most widely is dicationic quaternary ammonium geminis, which is denote as C_M–C_S–C_M [15,16]. The headgroup of gemini surfactant molecule usually affects the aggregation behavior, the surface and bulk properties [17,18]; the spacer group governs the separation distance between the head groups, and thus influences the packing geometry and mobility of the surfactant [19,20]. Considering the good characteristics of gemini surfactants over conventional surfactants, Li et al. used them to improve the electroactivity of proteins recently, and they obtained some interesting results [21].

In the present work, a novel HRP–polyvinyl alcohol (PVA)–C_{12}–C_{12}–C_{12} composite film is fabricated and studied electrochemically. In the composite film the heterogeneous electron-transfer rate of HRP is enhanced significantly. Therefore

* Corresponding author. Tel.: +86 2787218704.
E-mail addresses: bzzeng@whu.edu.cn, zengbz@chem.whu.edu.cn (B. Zeng).

0927-7765/$ – see front matter © 2008 Elsevier B.V. All rights reserved.
doi:10.1016/j.colsurfb.2008.09.018

it can present a pair of well-defined voltammetric peaks. The immobilized HRP also exhibits good electrocatalytic activity for the reduction of H_2O_2, NO_2^-, O_2, and trichloroacetic acid (TCA).

2. Experimental

2.1. Chemicals

HRP (>250 u mg^{-1}, M.W. 44,000) came from Beijing Biodee Biochemistry Co. Ltd. (Beijing, China). Its stock solution (5 mg ml^{-1}) was prepared by dissolving 5 mg HRP in 1.0 ml 0.10 M phosphate solution (PS, pH 5.0) and stored in a refrigerator. Cationic gemini surfactants dodecyl-α,ω-bis (dodecyldimethylammonium bromide) ($C_{12}H_{25}N(CH_3)_2$–$C_{12}H_{24}$–$N(CH_3)_2C_{12}H_{25}Br_2$, C_{12}–C_{12}–C_{12}), etc. were synthesized and purified according to literature [22]. The stock solutions of C_{12}–C_{12}–C_{12}, $C_{12}H_{25}N(CH_3)_2$–C_4H_8–$N(CH_3)_2C_{12}H_{25}Br_2$ (C_{12}–C_4–C_{12}), $C_{12}H_{25}N(CH_3)_2$–C_4H_7OH–$N(CH_3)_2C_{12}H_{25}Br_2$ (C_{12}–C_4OH–C_{12}), $C_{12}H_{25}N(CH_3)_2$–CH_2–C_6H_4–CH_2–$N(CH_3)_2C_{12}H_{25}Br_2$ (C_{12}–ph–C_{12}) were prepared with redistilled water. PVA was purchased from Sinopharm Chemical Reagent Co. Ltd. (Shanghai, China). PVA aqueous solution (3 mg ml^{-1}) was prepared by dissolving 30 mg PVA in 10 ml warm redistilled water (80 °C) and stored in a refrigerator. Hydrogen peroxide was product of Sinopharm Chemical Reagent Co. Ltd. Other reagents used were of reagent or of analytical grade. Water used in all experiments was redistilled.

2.2. Preparation of modified electrode

Before modification, the glassy carbon electrodes (GCEs, Ø2 mm) were polished on a polishing pad with 0.05 μm alumina slurry, rinsed with water, ultrasonicated for 1 min in redistilled water, and dried in air. The effective area of the GC was estimated to be 0.0116 cm^2 according to the method described in literature [23]. HRP–PVA–C_{12}–C_{12}–C_{12} mixture was made by mixing 5 mg ml^{-1} HRP solution, 3 mg ml^{-1} PVA solution and 0.010 M C_{12}–C_{12}–C_{12} solution in a plastic tube with the aid of ultrasonic agitation, and their volume ratio is 2:1:1. Four microliters of the mixture were transferred onto the cleaned GC electrode with a microsyringe, and then let it dry at room temperature. The resulting electrode was denoted as HRP–PVA–C_{12}–C_{12}–C_{12}/GC. For comparison, HRP–PVA–C_{12}–C_4–C_{12}/GC, HRP–PVA–C_{12}–C_4OH–C_{12}/GC, HRP–PVA–C_{12}–ph–C_{12}/GC, HRP–PVA/GC (without C_{12}–C_{12}–C_{12}), HRP/GC (without C_{12}–C_{12}–C_{12} and PVA) and PVA–C_{12}–C_{12}–C_{12}/GC (without HRP) were also prepared through similar procedure. The electrodes were stored at 4 °C when they were not used.

2.3. Apparatus and experimental procedure

Electrochemical measurements were performed with a CHI 617 electrochemical workstation (CH Instrument Company, Shanghai, China) and a conventional three-electrode system. The modified electrode served as working electrode, a platinum wire as counter electrode, and a saturated calomel electrode (SCE) as reference electrode. A 0.10 M pH 7.0 phosphate buffer solution (PBS) was used as supporting electrolyte. Prior to measurement the electrolyte solution was deaerated with nitrogen gas for 30 min, and a nitrogen atmosphere was maintained over the electrochemical cell during the experiment. All experiments were carried out at room temperature. UV–vis absorption spectra were recorded with a TU-1901 UV–vis spectrophotometer (Purkinje General Instrument Co. Ltd., Beijing, China). For spectrum measurement, HRP solution, HRP–PVA–C_{12}–C_{12}–C_{12} solution and PVA–C_{12}–C_{12}–C_{12} solution were dropped on quartz glass slides and dried in air, respectively.

3. Results and discussion

3.1. UV–vis absorption spectra of composite film

The UV–vis spectra of HRP film and HRP–PVA–C_{12}–C_{12}–C_{12} film on quartz glass slides are shown in Fig. 1. The HRP exhibits an absorption peak at 398 nm, while the HRP–PVA–C_{12}–C_{12}–C_{12} presents an absorption peak at 400 nm. Their peak shape is almost same, in addition to the slight difference of peak absorbance and peak wavelength. The small difference can be ascribed to the weak interaction between HRP and PVA–C_{12}–C_{12}–C_{12}. As the absorption curve of HRP keeps almost unchanged when it is immobilized in the PVA–C_{12}–C_{12}–C_{12}, it is thought that the HRP may remain native structure.

3.2. Voltammetric behavior of HRP in PVA–C_{12}–C_{12}–C_{12} film

Fig. 2 shows a typical cyclic voltammogram of HRP–PVA–C_{12}–C_{12}–C_{12}/GC in PBS. A pair of well-defined peaks is observable. Their peak-potential separation (ΔE_p) is 56 mV and the formal potential ($E^{O'}$) is −0.214 V. The ratio of anodic peak current and cathodic peak current is close to 1. Therefore, the electrochemical process is quasi-reversible. The redox peaks undoubtedly result from the redox of Fe(III)/Fe(II) couple of HRP, since the PVA–C_{12}–C_{12}–C_{12}/GC cannot produce such redox peaks [24]. The HRP/GC and PVA–HRP/GC electrodes can also exhibit a pair of redox peaks, respectively, but their peaks are much smaller and asymmetric in comparison with that of HRP–PVA–C_{12}–C_{12}–C_{12}/GC. Hence it can be proposed that C_{12}–C_{12}–C_{12} could enhance the electron transfer rate between HRP and the underlying electrode and make more HRP molecules participate in electrode reaction. This is related to the fine biocompatibility of C_{12}–C_{12}–C_{12}. In addition, the cationic gemini surfactant may act as electron-conducting tunnel [25,26]. In this case the surface concentration of electroactive HRP (Γ^*) for the HRP–PVA–C_{12}–C_{12}–C_{12}/GC is estimated according to the equation $Q = nFA\Gamma^*$ [27], and it is 1.49×10^{-10} mol cm^{-2}, supposing that the electrochemical reaction includes 1e transfer. As the theoretical value of monolayer coverage of HRP is about

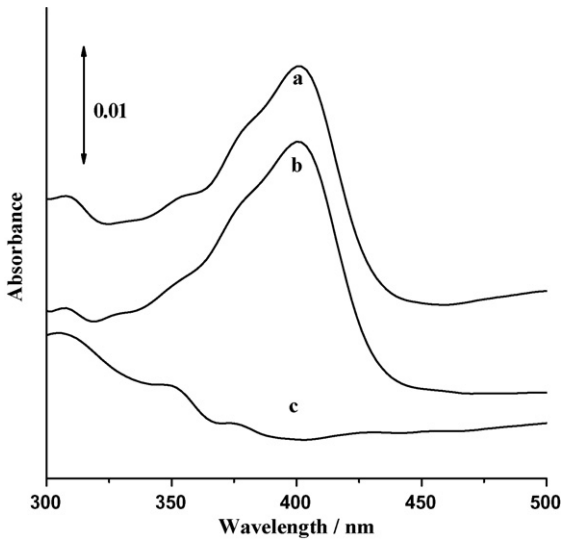

Fig. 1. UV–vis absorption spectra of HRP–PVA–C_{12}–C_{12}–C_{12} (a), HRP (b), and PVA–C_{12}–C_{12}–C_{12} (c) in 0.10 M pH 7.0 PBS.

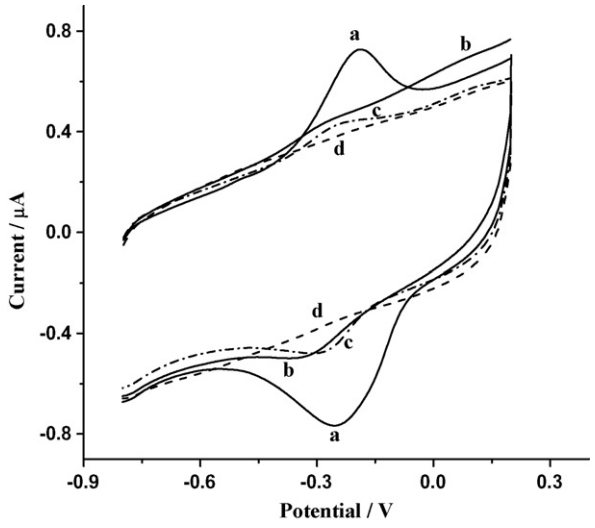

Fig. 2. Cyclic voltammograms of HRP–PVA–C_{12}–C_{12}–C_{12}/GC (a), HRP/GC (b), HRP–PVA/GC (c) and PVA–C_{12}–C_{12}–C_{12}/GC (d) in 0.10 M pH 7.0 PBS. Scan rate: 0.2 V s^{-1}.

5.1×10^{-11} mol cm^{-2} [28], the experimental value is much higher than the theoretical one. Thus multilayer of HRP must participate in the electrode reaction. The percentage of electroactive HRP on the electrode surface is about 0.76%. This indicates that only a small part of immobilized HRP can exchange electron with the electrode. It should be pointed out that the HRP–C_{12}–C_{12}–C_{12}/GC is unstable due to the weaker adherence of the HRP–C_{12}–C_{12}–C_{12} composite to GC electrode; hence PVA is introduced to immobilize the composite. PVA almost does not affect the HRP peaks if its concentration is small.

3.3. Influence of different gemini surfactants

In order to study the influence of different gemini surfactants on the electrochemical activity of HRP, other three gemini surfactants are tested, including C_{12}–C_4–C_{12}, C_{12}–C_4OH–C_{12}, and C_{12}–ph–C_{12}. As shown in Fig. 3, C_{12}–C_4–C_{12} and C_{12}–ph–C_{12} show weak effect in promoting the electron transfer of HRP, while C_{12}–C_4OH–C_{12} makes

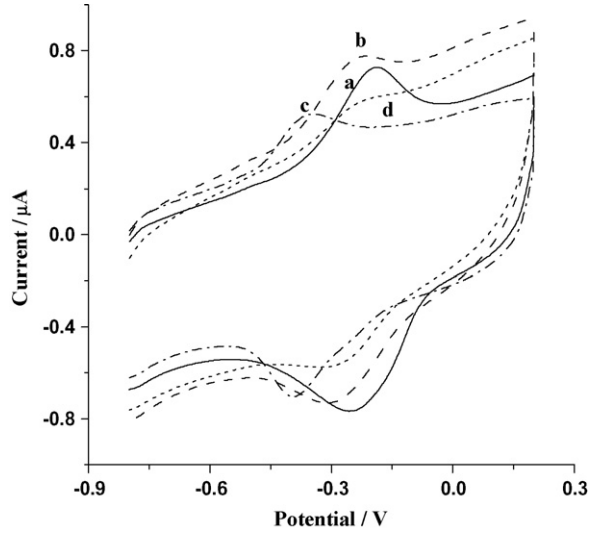

Fig. 3. Cyclic voltammograms of different HRP–PVA–gemini surfactant/GC. Geminis: C_{12}–C_{12}–C_{12} (a), C_{12}–C_4–C_{12} (b), C_{12}–C_4OH–C_{12} (c), and C_{12}–ph–C_{12} (d). Scan rate: 0.2 V s^{-1}; other conditions as in Fig. 2.

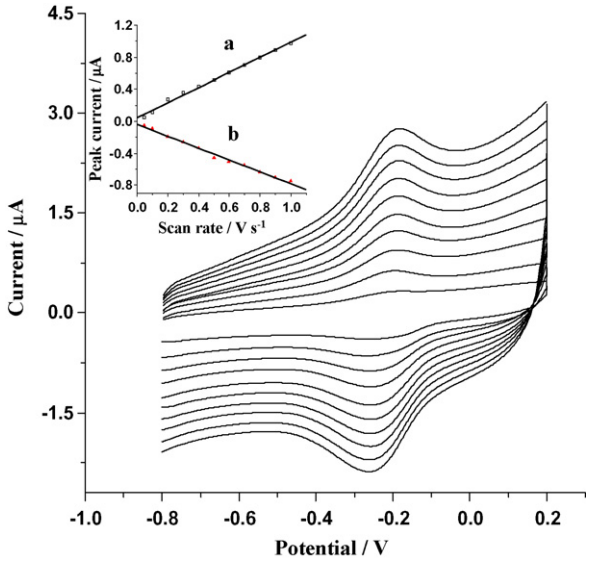

Fig. 4. Influence of scan rate on peak current and peak potential of HRP–PVA–C_{12}–C_{12}–C_{12}/GC in 0.10 M pH 7.0 PBS. Scan rate: 0.1, 0.2, 0.3, 0.4, 0.5, 0.6, 0.7, 0.8, 0.9, and 1.0 V s^{-1} (from inner to outer); inset: plots of anodic peak current (a) and cathodic current (b) vs. scan rate.

the HRP peaks more reversible and higher. However, in comparison with C_{12}–C_4OH–C_{12}, C_{12}–C_{12}–C_{12} is more suitable for improving the direct electron transfer. In addition, the peak potentials change with gemini surfactant, meaning that the surfactant also influences the activation energy of HRP molecule. As the alkyl chains of these gemini surfactants are same, their different effect should be ascribed to the different action of their spacers. It is mentioned previously that the spacer group influences the packing geometry and mobility of gemini surfactant [19,20]. Hence, it is thought that the electroactivity of HRP is related to the micelle structure of gemini surfactants, which affects the interaction between HRP and gemini surfactant. This implies that the electroactivity of HRP can be adjusted through changing spacer group, which is different from conventional single-chain surfactant. Here, the –C_4–, –C_4OH– and –ph– groups are more rigid, the –C_{12}– group is more flexible, and –C_4OH– group is more hydrophilic. Accordingly, it seems that the spacer group with higher flexibility and hydrophility is favorable to the electron transfer.

3.4. Influence of scan rate

The influence of scan rate on the voltammetric peaks of HRP–PVA–C_{12}–C_{12}–C_{12}/GC is shown in Fig. 4. The anodic peak current and cathodic peak current both change linearly with scan rate in the range studied (i.e. 0.05–1 V s^{-1}), and the regression equations are: $i_{pa} = 0.935\,\nu + 0.072$ (i_{pa}: μA, ν: V s^{-1}, $r = 0.998$) and $i_{pc} = -0.740\,\nu - 0.0435$ (i_{pc}: μA, ν: V s^{-1}, $r = 0.997$). The slope ratio of the $\lg i_p$ vs. $\lg \nu$ plots is close to 1, and the charge (Q, i.e. the peak area) values are independent of scan rate. These reflect the features of a thin-layer system. With increasing the scan rate, the anodic peak shifts positively and the cathodic peak shifts negatively, thus ΔE_p increases. It indicates that the electron-transfer rate of HRP is not very fast.

3.5. Influence of solution pH

The HRP immobilized on the PVA–C_{12}–C_{12}–C_{12} film shows well-defined redox peaks in the pH range of 3.0–11.0. The peak current increases with pH changing from 3.0 to 7.0, and then it decreases rapidly upon further raising pH (Fig. 5). This means that the

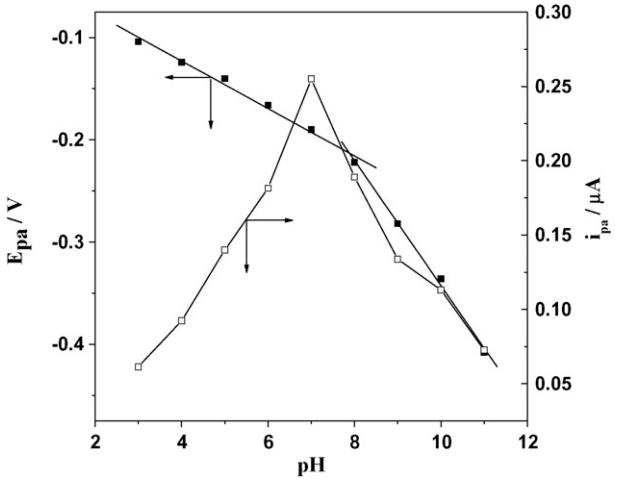

Fig. 5. Influence of pH on anodic peak current and peak potential of HRP–PVA–C_{12}–C_{12}–C_{12}/GC. Other condition as in Fig. 2.

HRP–PVA–C_{12}–C_{12}–C_{12} film has higher electroactivity in neutral solutions, which is well accordance with the higher bioactivity of enzyme. The peak potentials of HRP strongly depend on pH. In the pH range of 3.0–8.0, the anodic peak potential of HRP shifts negatively at a rate of $-23.3\,mV\,pH^{-1}$, but it becomes $-61.2\,mV\,pH^{-1}$ over the range of pH 8–11. This indicates that the electrochemical process involves proton transfer. As to the difference, it can be ascribed to the influence of the protonization of HRP [27].

3.6. Electrocatalytic action of immobilized HRP

Fig. 6 displays the cyclic voltammogram of HRP–PVA–C_{12}–C_{12}–C_{12}/GC in H_2O_2 solution. As expected, when H_2O_2 is introduced into the solution the cathodic peak current increases significantly. Meanwhile, the anodic peak current decreases gradually. As PVA–C_{12}–C_{12}–C_{12}/GC cannot show such phenomenon, it can be inferred that the HRP catalyzes the reduction of H_2O_2. With H_2O_2 concentration changing the cathodic peak current changes linearly with it in the range of 0.195–97.5 μM, and the regression equation is: $i_{pc} = -0.254 - 0.00755c$ (i_{pc}: μA, c: μM, $r = 0.997$). The detection limit is estimated to be 6.5×10^{-8} M, which is lower than that of other H_2O_2 biosensors based on HRP-modified electrodes [29]. When the concentration of H_2O_2 exceeds 97.5 μM, the cathodic peak current almost stops increasing, implying that the catalysis capacity of the HRP–PVA–C_{12}–C_{12}–C_{12}/GC is limited. This also reflects the feature of Michaelis–Menten response. According to the Lineweaver–Burk equation [29]:

$$\frac{1}{I_{ss}} = \frac{1}{I_{max}} + \frac{K_m}{I_{max}c}$$

where I_{ss} is the catalytic current after the addition of H_2O_2; I_{max} is the maximum catalytic current measured under saturated H_2O_2 conditions; c is the bulk concentration of the substrate and K_m is Michaelis–Menten constant. In this case, the apparent I_{max} and K_m are derived from the plot of the $1/I_{ss}$ vs. $1/c$, and they are 2.05 μA and 110.5 μM, respectively. The smaller K_m value indicates the higher electrocatalytic efficiency of the HRP–PVA–C_{12}–C_{12}–C_{12}/GC to the reduction of H_2O_2 [30–32].

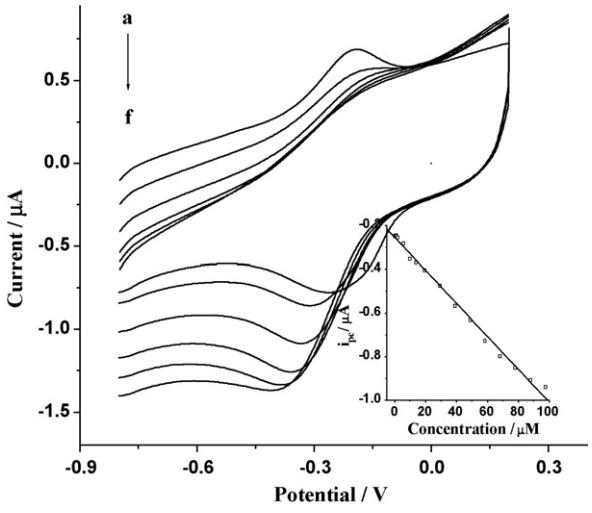

Fig. 6. Cyclic voltammograms of HRP–PVA–C_{12}–C_{12}–C_{12}/GC in 0.10 M pH 7.0 PBS-containing H_2O_2. H_2O_2 concentration: (a) 0 μM, (b) 19.5 μM, (c) 39 μM, (d) 58.5 μM, (e) 78 μM, and (f) 97.5 μM; scan rate: $0.2\,V\,s^{-1}$; inset: plot of catalytic peak current vs. H_2O_2 concentration.

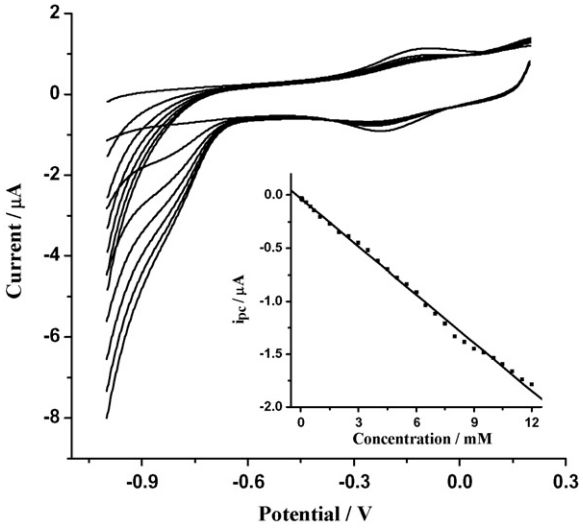

Fig. 7. Electrocatalytic reduction of NO_2^- at PVA–C_{12}–C_{12}–C_{12}–HRP/GC in 0.10 M pH 5.0 PS. NO_2^- concentration: 0, 3.5, 5.5, 7.5, 9.5 and 11.5 mM (from inner to outer); scan rate: $0.2\,V\,s^{-1}$; inset: plot of catalytic peak current vs. NO_2^- concentration.

The electrocatalytic activity of HRP–PVA–C_{12}–C_{12}–C_{12}/GC toward oxygen (O_2) reduction is also investigated. The catalytic reduction peak of O_2 is similar to that of H_2O_2. It implies that the electrochemical reduction mechanisms of O_2 and H_2O_2 have some intrinsic relation [33]. In addition, the HRP–PVA–C_{12}–C_{12}–C_{12}/GC can catalyze the reduction of NO_2^- and TCA (Fig. 7). When NO_2^- solution is added to the bulk solution, a new reduction peak occurs at −0.75 V. The peak current increases linearly with NO_2^- concentration from 0.03 to 12 mM, and the regression equation is: $i_{pc} = -0.0302 - 0.151c$ (i_{pc}: μA, c: mM, $r = 0.998$). Meanwhile, the cathodic peak current of HRP decreases slightly, compared with that without NO_2^-. The response of NO_2^- also exhibits the characteristic of Michaelis–Menten response, the apparent Michaelis–Menten constant K_m is estimated to be 49.7 mM. As to TCA, the catalytic peak current is linear to its concentration over the range of 0.02–10 mM. The corresponding apparent Michaelis–Menten constant K_m is ca. 5.66 mM.

3.7. Reproducibility and stability of HRP–PVA–C_{12}–C_{12}–C_{12}/GC

To explore the reproducibility of the HRP–PVA–C_{12}–C_{12}–C_{12} film-coated electrode, the cyclic voltammograms of five different electrodes are recorded. As a result, the relative standard deviation

of the anodic peak current of HRP is about 6.5%. When an electrode was cycled consecutively between 0.2 and −0.8 V for 200 times, the peak current decreases by 5.7%. The anodic peak current of the HRP–PVA–C_{12}–C_{12}–C_{12}/GC decreases by less than 5% after storing for 1 week at 4 °C. This indicates that the HRP immobilized in the PVA–C_{12}–C_{12}–C_{12} composite is stable and such electrode is easily replicated [34].

4. Conclusions

A novel PVA–C_{12}–C_{12}–C_{12} composite film is prepared. The film can provide a favorable microenvironment for HRP. HRP shows higher heterogeneous electron-transfer rate in it. The immobilized HRP thus can exhibit a pair of quasi-reversible voltammetric peaks. It also possesses good electrocatalytic activity to the reduction of H_2O_2, NO_2^-, O_2, and TCA. The electroactivity of HRP suffers some effect from the spacer group of gemini surfactant. Through changing the spacer group the electroactivity of HRP can be adjusted. In addition, with the protection of polyvinyl alcohol the resulting HRP electrode shows better stability. Accordingly, such gemini surfactant-based composite has potential application in immobilizing proteins.

Acknowledgement

The authors appreciate the support of the National Nature Science Foundation of China (No. 20173040).

References

[1] P.A. Mabrouk, Anal. Chim. Acta 307 (1995) 245.
[2] S.Q. Liu, H.X. Ju, Anal. Biochem. 307 (2002) 110.
[3] E.E. Ferapontova, Electroanalysis 16 (2004) 1101.
[4] A.K.M. Kafi, D.Y. Lee, S.H. Park, Y.S. Kwon, Microchem. J. 85 (2007) 308.
[5] J.F. Rusling, A.F. Nassar, J. Am. Chem. Soc. 155 (1993) 11891.
[6] J.W. Li, C. Fan, F. Xiao, R. Yan, S.S. Fan, F.Q. Zhao, B.Z. Zeng, Electrochim. Acta 52 (2007) 6178.
[7] X. Gan, T. Liu, J. Zhong, X. Liu, G. Li, Chembiochem 5 (2004) 1686.
[8] T. Hoshi, J.I. Anzai, T. Osa, Anal. Chem. 67 (1995) 770.
[9] X.J. Liu, Y.X. Huang, L.B. Shang, X.Y. Wang, H. Xiao, G.X. Li, Bioelectrochemistry 68 (2006) 98.
[10] H.J. Chen, S.J. Dong, Biosens. Bioelectr. 22 (2007) 1811.
[11] R. Yan, J.W. Li, F.Q. Zhao, B.Z. Zeng, Electrochim. Acta 52 (2007) 7425.
[12] J.F. Rusling, A.E.F. Nassar, J. Am. Chem. Soc. 115 (1993) 11891.
[13] O. Zheng, J.X. Zhao, J. Colloid Interf. Sci. 300 (2006) 749.
[14] C. McGregor, C. Perrin, M. Monck, P. Camilleri, A.J. Kirby, J. Am. Chem. Soc. 123 (2001) 6215.
[15] Y. Wang, E.F. Marques, J. Phys. Chem. B 110 (2006) 1151.
[16] G. Ronsin, C. Perrin, P. Guédat, A. Kremer, P. Camilleri, A.J. Kirbya, Chem. Commun. (2001) 2234.
[17] D. Danino, Y. Talmon, R. Zana, Langmuir 11 (1995) 1448.
[18] L.M. Colosi, Q.G. Huang, W.J. Weber, J. Am. Chem. Soc. 128 (2006) 4041.
[19] S. De, V.K. Aswal, P.S. Goyal, S. Bhattacharya, J. Phys. Chem. B 102 (1998) 6152.
[20] X.Y. Wang, J.B. Wang, Y.L. Wang, H.K. Yan, P.X. Li, R.K. Thomas, Langmuir 20 (2004) 53.
[21] J.W. Li, L.H. Liu, F. Xiao, F.Q. Zhao, B.Z. Zeng, J. Electroanal. Chem. 613 (2008) 51.
[22] M.J. Rosen, L.D. Song, J. Colloid Interf. Sci. 179 (1996) 261.
[23] A.J. Bard, L.R. Faulkner, Electrochemical Methods: Fundamentals and Applications, 2nd ed., John Wiley & Sons, Inc., New York, 1980, pp. 27–45, 211, 231, 594.
[24] P.N. Bartlett, P.R. Birkin, J.H. Wang, Anal. Chem. 70 (1998) 3685.
[25] G. Ronsin, C. Perrin, P. Guédat, A. Kremer, P. Camilleri, A.J. Kirby, Chem. Commun. (2001) 2234.
[26] A.J. Bard, Electroanalytical Chemistry, Marcel Dekker, New York, 1986, p. 13, 191.
[27] S.F. Wang, T. Chen, Z.L. Zhang, X.C. Shen, Z.X. Lu, D.W. Pang, K.Y. Wong, Langmuir 21 (2005) 9260.
[28] I. Yamazaki, T. Arisso, Y. Hayashi, H. Yamada, R. Makino, Adv. Biophys. 11 (1978) 249.
[29] R. Oda, I. Huc, J.C. Homo, B. Heinrich, M. Schmutz, S. Candau, Langmuir 15 (1999) 2385.
[30] H. Huang, N.F. Hu, Y.H. Zeng, G. Zhou, Anal. Biochem. 308 (2002) 141.
[31] F.X. Gao, R. Yuan, Y.Q. Chai, S.H. Chen, S.R. Cao, M.Y. Tang, J. Biochem. Biophys. Methods 70 (2007) 407.
[32] R.A. Kamin, G.S. Willson, Anal. Chem. 52 (1980) 1198.
[33] T. Ferri, A. Poscia, R. Santucci, Bioelectrochem. Bioenerg. 45 (1998) 221.
[34] X.B. Lu, Q. Zhang, L. Zhang, J.H. Li, Electrochem. Commun. 8 (2006) 874.